
This is an electronic reprint of the original article.
This reprint may differ from the original in pagination and typographic detail.

Lucenius, Jessica; Valle-Delgado, Juan José; Parikka, Kirsti; Österberg, Monika
Understanding hemicellulose-cellulose interactions in cellulose nanofibril-based composites

Published in:
Journal of Colloid and Interface Science

DOI:
[10.1016/j.jcis.2019.07.053](https://doi.org/10.1016/j.jcis.2019.07.053)

Published: 20/07/2019

Document Version
Publisher's PDF, also known as Version of record

Published under the following license:
CC BY

Please cite the original version:
Lucenius, J., Valle-Delgado, J. J., Parikka, K., & Österberg, M. (2019). Understanding hemicellulose-cellulose interactions in cellulose nanofibril-based composites. *Journal of Colloid and Interface Science*, 555, 104-114. <https://doi.org/10.1016/j.jcis.2019.07.053>

This material is protected by copyright and other intellectual property rights, and duplication or sale of all or part of any of the repository collections is not permitted, except that material may be duplicated by you for your research use or educational purposes in electronic or print form. You must obtain permission for any other use. Electronic or print copies may not be offered, whether for sale or otherwise to anyone who is not an authorised user.



Contents lists available at ScienceDirect

Journal of Colloid and Interface Science

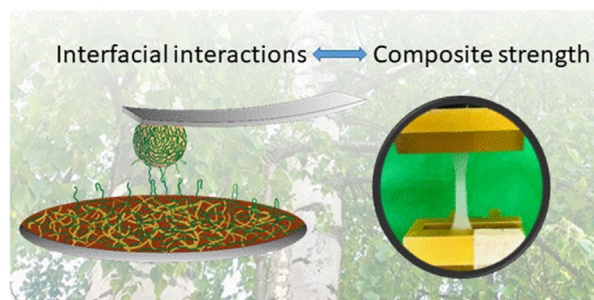
journal homepage: www.elsevier.com/locate/jcis

Regular Article

Understanding hemicellulose-cellulose interactions in cellulose nanofibril-based composites

Jessica Lucenius^a, Juan José Valle-Delgado^{a,*}, Kirsti Parikka^b, Monika Österberg^{a,*}^a Department of Bioproducts and Biosystems, School of Chemical Engineering, Aalto University, FI-00076 Aalto, Finland^b Department of Food and Environmental Sciences, University of Helsinki, FI-00014 Helsinki, Finland

GRAPHICAL ABSTRACT



ARTICLE INFO

Article history:

Received 10 June 2019

Revised 16 July 2019

Accepted 20 July 2019

Available online 20 July 2019

Keywords:

Cellulose nanofibrils

Hemicellulose

Biocomposites

Surface forces

Friction

Colloidal probe microscopy (CPM)

Quartz crystal microbalance with

dissipation (QCM-D)

Wet strength

ABSTRACT

Plant-based polysaccharides (cellulose and hemicellulose) are a very interesting option for the preparation of sustainable composite materials to replace fossil plastics, but the optimum bonding mechanism between the hard and soft components is still not well known. In this work, composite films made of cellulose nanofibrils (CNF) and various modified and unmodified polysaccharides (galactoglucomannan, GGM; hydrolyzed and oxidized guar gum, GGhydHox; and guar gum grafted with polyethylene glycol, GG-g-PEG) were characterized from the nano- to macroscopic level to better understand how the interactions between the composite components at nano/microscale affect macroscopic mechanical properties, like toughness and strength. All the polysaccharides studied adsorbed well on CNF, although with different adsorption rates, as measured by quartz crystal microbalance with dissipation monitoring (QCM-D). Direct surface and friction force experiments using the colloidal probe technique revealed that the adsorbed polysaccharides provided repulsive forces—well described by a polyelectrolyte brush model – and a moderate reduction in friction between cellulose surfaces, which may prevent CNF aggregates during composite formation and, consequently, enhance the strength of dry films. High affinity for cellulose and moderate hydration were found to be important requirements for polysaccharides to improve the mechanical properties of CNF-based composites in wet conditions. The results of this work provide fundamental information on hemicellulose-cellulose interactions and can support the development of polysaccharide-based materials for different packaging and medical applications.

© 2019 Published by Elsevier Inc.

1. Introduction

The research field of nanocellulose and nanocellulose based composites has been growing exponentially during the past decade. One of the most tempting approaches is to create

* Corresponding authors.

E-mail addresses: juanjose.valledelgado@aalto.fi (J.J. Valle-Delgado), monika.osterberg@aalto.fi (M. Österberg).

biocomposites from nanocellulose, hemicelluloses, and mannans to replace fossil-based materials, and to be used for high-end applications.

Hemicelluloses are short-chain polysaccharides bound to cellulose in plant cell walls [1]. In the plant cell wall the cellulose molecules are assembled into long fibrils and the fibrils are assembled into layers with systematic order and packed together into larger fibers. The hemicelluloses are located on the cellulose fibril surface and bind the cellulose together with lignin. The cellulose fibrils and fibers provide structural support to plants and are responsible for wood strength. Cellulose pulp can be obtained from plant cell walls, and wood-based cellulose nanofibrils (CNF) can be obtained from cellulose pulp by mechanical disintegration, usually combined with chemical or enzymatic treatments [2]. The nanocelluloses obtained are structures with dimensions of few nanometers in width and from tens of nanometers to a few micrometers in length.

Cellulose and hemicellulose (interfacial) interactions in the cell wall play an important role in the excellent tensile properties (e.g. flexibility) of wood-based materials [1]. Few research groups so far have addressed the need to understand these interactions. Nevertheless, a deeper understanding of cellulose-hemicellulose interactions and how polysaccharide modifications affect those interactions would aid the design of tailored composites with optimal properties [3,1]. Seminal studies in the topic often include model surface adsorption studies using the quartz crystal microbalance with dissipation monitoring (QCM-D) combined with interfacial interaction studies using colloidal probe microscopy (CPM) [4,5,6,3]. In these studies, it has been noted that DLVO theory (formulated by Derjaguin, Landau, Verwey, and Overbeek, it considers that the interactions between two charged surfaces in a medium can be described as a sum of the van der Waals forces and the electrostatic double layer forces) explains quite well the interactions in simple systems such as forces between two cellulose surfaces [7,8]. In cases where adsorbed polymers are present, DLVO theory has been used to explain the long-range decay of the force profile by assigning the plane of charge to suitable separation [4]; however, short-range interactions in these systems have often been explained only qualitatively, and generally attributed to steric interactions.

Cellulose, and CNF in particular, is considered to have substantial potential in packing and medical applications [9,10]. Hemicelluloses are used as filler material and dietary fibers in the pharmaceutical and food industries and they are good binders and stabilizers in paper manufacturing [11]. The preparation of natural polysaccharide-cellulose composites, where CNF is used as a reinforcing component, has been investigated for the replacement of synthetic polymers in different biomimetic approaches [12,13,14,15,16]. In order to enhance the composite properties (stiffness and toughness) and compatibility between the components, the polysaccharides have often been chemically modified following different strategies, for example, TEMPO-mediated oxidation [17]. Water soluble polysaccharides from plants have also been combined with calcium phosphate or acrylamide to obtain scaffolds for bone regeneration or materials with improved thermal stability, respectively [18,19].

Despite the interest in CNF and hemicellulose based nanocomposites and the importance of cellulose-hemicellulose binding in the plant cell wall, there is a lack of understanding of the interactions between these biopolymers, and more specifically, how these interactions correlate with mechanical properties of bionanocomposites. Hence, the interactions of CNF with several water-soluble polysaccharides subjected to different modifications are studied in this work, and the results are compared with previously published works to unravel the factors affecting cellulose-hemicellulose binding. The adsorption of galactoglucomannan

(GGM), hydrolyzed and oxidized guar gum (GGhydHox), and guar gum grafted with polyethylene glycol (GG-g-PEG), on CNF thin films was studied by QCM-D. The interaction forces and friction of these polysaccharides with cellulose surfaces at micro/nanoscale were analyzed by CPM using an atomic force microscope. The mechanical properties of free standing polysaccharide-CNF films were also characterized using tensile testing as an attempt to correlate the interactions at micro/nanoscale with the macroscopic properties of composites. Here we have chosen to use galactose oxidase [20] for the oxidation of GG, since it is often used in hydrogels and in aerogels with CNF [21]. The information gathered in this work can support the design and optimization of new, environmentally friendly, polysaccharide-based materials.

2. Materials and methods

2.1. Materials

Cellulose nanofibrils (CNF) were prepared from never dried birch pulp from a Finnish pulp mill. The pulp was washed to sodium form [22] in order to control the ionic strength and counter ion type prior to disintegration. Next the pulp was fluidized using a fluidizer (Microfluidics, M-110Y, Microfluidics Int. Co., Newton, MA). For free-standing films, the pulp was circulated six times through the fluidizer, while for the thin films for QCM-D and CPM experiments, up to 20 passes were used. The carbohydrate composition of the pulp was 72,8% glucose, 25,6% xylose and 1,4% mannose and the charge was approximately 65 $\mu\text{eq/g}$. The CNF is expected to have the same composition as the pulp. The zeta potential of the CNF was around 2–3 mV [23,24].

Spruce galactoglucomannan (GGM, *Picea abies*, Mw 60 kDa) was obtained from the process water of a Finnish pulp mill in an industrial-scale isolation trial after ethanol precipitation. Prior to use, the GGM was dissolved in water at 80 °C and the solution was then cooled to room temperature, stirred overnight, and filtered using glass microfiber filters (Whatman, Scheicher & Schnell Cat No. 1820 125). The GGM sample was industrial grade with following sugar- and acid content in mole percent's: arabinose 3.4%, galactose 13%, glucose 18%, xylose 1.4%, mannose 58%, rhamnose 0.1%, galacturonic acid 4.1%, glucuronic acid, 4-O-methyl glucuronic acid 0.2%. The degree of acetylation was 14% [25].

Guar gum (GG) was purchased from Sigma Aldrich (Lot#041M0058V, Pcode 10011170894). The molecular weight was ≥ 1000 kDa and total ash content <1%. 12 mM sodium phosphate buffer, pH 6.2 was used for the AFM and QCM-D experiments.

2.2. Hydrolysis and oxidation of GG

Guar gum (GG) was used after enzymatic modifications: partial hydrolysis and oxidation. The partial hydrolysis was performed with endo-1,4- β -mannanase (EC number 3.2.1.78, Lot 00803, from *Aspergillus niger*, 42 U/mg) from Megazyme (Wicklow, Ireland).

The partially hydrolyzed GG was prepared as explained in Lucenius, Parikka et al. [12]. GG was dissolved to obtain 1.0% (w/v) solution in 0.1 M sodium acetate buffer, pH 5, and endo-1,4- β -mannanase was added (0.6 mU/mg of GG). The solution was incubated in a water bath for 4 h at 40 °C, followed by heating at 100 °C for 10 min to inactivate the enzyme, after which the samples were centrifuged at 5000 rpm and the supernatant was collected, freeze dried and used for the studies. Hereafter the names of the samples are abbreviated as follows: partially hydrolyzed GG (GGhyd) and hydrolyzed, low oxidized GG (GGhydLox) and highly oxidized GG (GGhydHox). Size exclusion chromatography (SEC) (OHpak SB-806 M HQ, 8 \times 300 mm, exclusion limit

2×10^7 , Showa Denko, Ogimachi, Japan) was used to characterize the molar mass of GGhyd [26]. GGhyd was dissolved in 0.1 M NaNO₃. Molar mass was calculated using a dn/dc value of 0.15 ml/g. The molar mass of hydrolyzed GG was approximately 30 kDa and the hydrodynamic radius of the sample (R_h) was 4.7 nm.

The partially hydrolyzed GG (GGhyd) was then oxidized by Galactose oxidase (GO; G7400, 3685 U/g, Lot# 05K8601, Sigma-Aldrich St. Louis, MO, U.S.A., Fig. 1). Catalase (from bovine liver, C30, 22,000 U/mg, Lot# 20M7008V, Sigma-Aldrich St. Louis, MO, U.S.A.), and horseradish peroxidase (P8250, type II, 181 U/mg, Lot# 20M7008V, Sigma-Aldrich St. Louis, MO, U.S.A.) were used to catalyze the reaction. The dosage of the enzymes was based on the approximate amount of galactose present in the GG sample, 1.50 U of GO, 150 U of catalase, and 0.9 U of HRP/mg of galactose. The 1% (w/v) solution of GGhyd was stirred in the presence of the enzymes at +4 °C for 48 h. The enzymes were inactivated by heating the sample up to 90 °C.

The degree of oxidation of GGhydLox was determined with gas chromatography mass spectrometry (GC-MS) by a method explained in detail in [26]. The degree of oxidization of GGhyd used for the synthesis of GGhyd grafted with PEG (GG-g-PEG) was ca. 30% for galactosyl residues and 15% for total carbohydrates. In the other experiments, GGhyd was used as prepared and with a variation of 28–30% degree of oxidation of total polysaccharides.

2.3. Synthesis of GG-g-PEG

Poly(ethylene glycol) monomethyl ether (mPEG), with an average molar mass of 5000 g/mol was obtained from Sigma-Aldrich Lot# BCB665776V. The hydroxylamine derivative of mPEG was synthesized according to a method described previously [27]. Diisopropyl azodicarboxylate (212 μ l) was added dropwise to a mixture of mPEG (2.0 g), *N*-hydroxyphtalimide (194 mg), and PPh₃ (312 mg) in dry dichloromethane (CH₂Cl₂) (10 ml) under nitrogen (N₂) atmosphere, and stirred for 24 h at RT. The solution was transferred to a bigger container and 250 ml of diethyl ether (Et₂O) was added, precipitating a white solid. After stirring the mixture for 20 min, the precipitate was collected by filtration and washed with three ca. 50 ml portions of Et₂O. The product was dried under reduced pressure. All chemicals were of analytical grade, if not otherwise stated.

The presence of the *N*-hydroxyphtalimide moiety was confirmed by ¹H NMR (supplementary data, Fig. S1)[27]; 400 MHz CDCl₃: δ 3.32 (3H, s), 3.4–3.8 (PEG chemical shifts), 7.70 (m, 2H), 7.76 (m, 2H). The product was then dissolved in CH₂Cl₂ (10 ml) and the phtalimide moiety was cleaved by adding hydrazine

hydrate (70 μ l) and stirring the mixture for 24 h at RT. A precipitate formed and the mixture was filtered. The solution containing the product was concentrated and dried under reduced pressure. The cleavage was confirmed by ¹H NMR [27]; 400 MHz CDCl₃: δ 3.4 (3H, s), 3.5–3.9 (PEG chemical shifts) (supplementary data, Fig. S2). To conjugate the product with GGhydLox (Fig. 1), GGhydLox (1.0 g, degree of oxidation 15%, ca. 0.0083 mol of aldehyde-containing galactosyl residues) was dissolved in 300 ml of 0.25 M sodium phosphate buffer (pH 5.8). The mPEG derivative (4.2 g; 0.0083 mol) was then added and the mixture stirred for 24 h. The product was then stored at 4 °C for further experiments. The formation of the oxime bond was confirmed by ¹H NMR [28]; 400 MHz D₂O): δ 3.3 (s, 3H), 3.4–4.2 (overlapping GG and PEG chemical shifts), 4.8–5.1 (GG chemical shifts), 6.8 (d, 0.1H), 7.5 (d, 0.5H) (supplementary data, Fig. S3). According to the comparison of the integral of the methoxy singlet to the combined integrals of the two oxime doublets the conversion to the oxime was ca. 65%. The degree of substitution with PEG moieties was estimated to be about 10%. GG-g-PEG was mixed with CNF suspension similarly as with other polymers in [12].

2.4. Preparation of free standing films

The CNF obtained after 6 passes through the fluidizer was diluted to 0.44% w/w suspension, and 0.84 g dry mass was used for each CNF film. The amount of CNF was the same in all composites. Low concentrations were used to avoid aggregation. For the preparation of composites films, additional polysaccharide was added to the CNF gel in concentrations of 2% and 10% of the dry mass of CNF and stirred and mixed according to the procedure described by Lucenius et al. [12]. The films were then wet-pressed and hot-pressed at 100 °C sequentially according to the method developed by Österberg, Vartiainen et al. [29].

2.5. Preparation of thin CNF films

Thin CNF films were deposited on QCM-D crystals (Biolin Scientific) by spin-coating as described in [30]. The crystals were first rinsed with Milli-Q water for 8 min, dried with nitrogen gas and cleaned in an ozonator (UV Ozone Cleaner-ProCleaner, Bioforce Nanosciences) for 20 min. After the cleaning, the crystals were immersed in polyethylene imine 1 g/L solution (PEI Mw, 50 000–100 000, Sigma Aldrich) for 1 h. The non-attached PEI was then washed away by gentle rinsing with Milli-Q water. The crystals were dried again with nitrogen gas and spin coated (WS-650 SX-6NPP/LITE Lavrell technologies corporation, North Wales, USA),

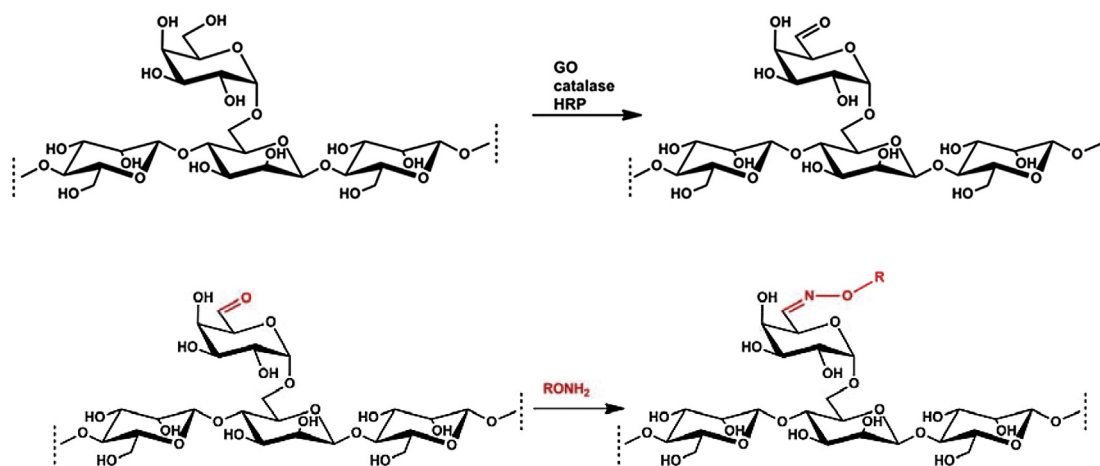


Fig. 1. The enzymatic oxidation of GGhyd (top) and synthesis of GG-g-PEG (bottom). R = polyethylene glycol moiety.

first with water (30 s) and then with CNF dispersion (1 min) at 3000 rpm [31]. The crystals were then dried in an oven at 80 °C for 20 min. Prior to the measurement, the CNF covered crystals were swollen with water in Petri dishes for 1 h. The CNF used to prepare thin films was similar to the one used to make free standing films, except that it was fluidized more extensively (up to 20 passes through the microfluidizer). 1.5 g CNF hydrogel (1.7% dry matter content) was first diluted with 12 ml of Milli-Q water and the solution ultrasonically defibrillated for 5 min (Branson Digital Sonifier D-450 for, 25% amplitude) to disperse the individual fibrils. The resulting CNF was then centrifuged (Beckman counter Optima Ultra centrifuge L-90 K, USA, New Boston) at 10400 rpm for 45 min, and top 5 ml of the supernatant (1.3 g/L) was used for spin coating

2.6. Quartz crystal microbalance with dissipation monitoring (QCM-D)

QCM-D is a very sensitive technique where the adsorption of a material on a quartz crystal is measured from the shift in the resonance frequency of the quartz crystal. The basic relationship between frequency shift and the absorbed mass is given by the Sauerbrey equation:

$$\Delta m_n = -\frac{CA\Delta f}{n} \quad (1)$$

where C is a device sensitivity constant (0.177 mg/m²) for a quartz resonator at 5 MHz, and n is the number of the frequency overtone. The Sauerbrey equation holds exactly only for rigid, sufficiently thin adsorbed layers and underestimates the absorbed mass in the case of viscoelastic films. However, this treatment was considered sufficient for the samples studied, as it gives realistic behavior for the adsorbed mass curve and the values are accurate enough for relative comparison between samples.

The viscoelastic nature of the adsorbed films cannot be determined from the frequency response alone. Thus, the dissipation of oscillator energy was measured simultaneously. The dissipation factor is defined as Eq. (2)

$$D = \frac{E_{\text{lost}}}{2\pi E_{\text{stored}}} \quad (2)$$

where E_{lost} is the energy lost during one oscillation cycle and E_{stored} is the total energy stored in the oscillator. Low and high dissipation factors indicate rigid and viscoelastic adsorbed films, respectively. The viscoelasticity can also be quantified by plotting dissipation as a function of frequency difference and calculating the slope of the resulting curve. The steeper the slope is, the more viscoelastic the adsorbed layer [32]. 0.1% polysaccharide solutions were prepared and stirred for several hours. The solutions were filtered through 1 μm glass filters and then diluted to concentrations of (300 ± 50) mg/L. All the solutions were fresh and prepared the same day of the measurements.

First, a flow of sodium phosphate buffer passed through the QCM-D chambers until a stable baseline was reached. Then the polysaccharide solutions were injected in the system at 100 μl/min for more than 1 h. Finally, the QCM-D chambers were rinsed with buffer for at least 1 h to remove loosely attached polysaccharides. At least two parallel measurements were carried out with exactly the same conditions.

2.7. Colloidal probe microscopy

Friction and surface forces between the cellulose surfaces and polysaccharide layers were measured in 12 mM sodium phosphate buffer utilizing a MultiMode 8 AFM (Bruker, Santa Barbara, CA) with the colloidal probe technique [33,34]. The AFM was equipped with a NanoScope V controller and a PicoForce scanner. Tipless

CSC12 and CSC38 probes (MikroMasch, Weztlar, Germany) were used in the force experiments. The lateral and vertical spring constants of the probes were determined by analyzing the thermal vibrations with the NanoScope 8.15 software and by using Sader's equations [35]. Values in the ranges 0.032–0.104 N/m and 1.0×10^9 – 2.45×10^9 N·m/rad were obtained for the vertical and lateral spring constants, respectively, for multiple experiments. After spring constant determination, the colloidal probes were prepared by gluing cellulose spheres with a radius of 14–19 μm at the end of the probes using a micromanipulator (Narishinge, Japan) and an UV-light curing adhesive (Norland Products Inc., Cranbury, USA). The dimensions of the colloidal probes were measured with a Leica DM400 optical microscope (Leica Microsystems, GmbH, Germany).

Friction and force measurements were carried out in two different regimes: (1), between the cellulose colloidal probes and polysaccharide layers previously adsorbed on CNF-coated QCM-D crystals; and (2), between the cellulose colloidal probes and CNF-coated QCM-D crystals before and after the adsorption of polysaccharides *in situ* in the AFM liquid cell (polysaccharide adsorption time of at least 50 min). For surface force measurements, the interacting surfaces were approached until contact and separated at a speed of 2 μm/s. The surface forces were calculated from the vertical deflection and vertical spring constant of the probes, and they were normalized by the radius of the colloidal probe. In friction force measurements, the colloidal probe slid over the flat substrate at a speed of 10 μm/s. The friction forces at 11 different applied loads (loading and unloading) were obtained from the lateral twist (average of 10 friction loops) and the lateral spring constant of the probes. The friction coefficients were obtained from the slope of the friction force-*versus*-applied load plots. The mean values of the friction coefficients from three measurements on three different spots of each sample and standard errors of the mean are provided.

Friction and force measurements were carried out on at least three different spots of each sample. At least 11 force curves were recorded on each spot before and after the corresponding friction measurement. The force and friction data were analyzed using ForceIT, FrictionIT and Matlab R1014b software. Representative force and friction curves are presented in this article. Both short and intermediate models were fitted simultaneously using a nonlinear least squares algorithm in Matlab® with the interaction scale, brush length and intermediate cut-off as fitting parameters; for the interaction scale, the only free variable is the area per charge.

2.8. Mechanical strength of free standing films

The CNF and CNF-polysaccharide free standing films were conditioned for at least 3 days at 23 °C and 50% RH before testing. Measurements of mechanical strength in both the dry and wet state were performed. The wet strength measurements were performed after 24 h soaking in Milli-Q water. The tensile mechanical properties of the films were measured using a MTS 400/M vertical tester (MTS System Corporation, Eden Prairie, USA), with a 200 N load cell (Adamel Lhomargy serial num. 115341, MTS). Bone shape strips with dimensions of 50 mm long, 5.3 mm wide and 60 ± 5 μm thick, were cut according to the procedure described in [36]. Before the tensile tests, the thickness of each film was measured at three different spots with a paper thickness meter (Lorentzen & Wettre, Kista, Sweden). The average thickness of these three different measurements was used to normalize the measured force when calculating the tensile stress. The grip distance was 40 mm and the testing velocity 0.5 mm min⁻¹. At least 5 parallel samples were tested and error bars illustrates the standard error of the mean value. The adjustable speed accuracy was 0.1% and the resolution for the crosshead displacement 0.01 mm.

3. Results and discussion

3.1. Adsorption of modified and unmodified hemicelluloses on CNF

The adsorption of modified and unmodified hemicelluloses on CNF model surfaces was studied by QCM-D. Fig. 2 shows the adsorption of hydrolyzed GG (GGhyd), hydrolysed oxidized GG (GGhydHox, degree of oxidation 24% total polysaccharide), GG-g-PEG, and GGM on CNF model surfaces measured by QCM-D. All the tested polysaccharides adsorbed well on CNF, but with different adsorption rates (Fig. 2a). The fastest adsorption was observed for GGhydHox, which had a higher affinity for CNF than GGhyd. The adsorbed GGhydHox layers were also the most dissipating ones (Fig. 2b). Unlike GGhyd, GGhydHox was observed to form gels (results not shown), indicating some crosslinking between the oxidized molecules, which could explain the higher adsorbed mass and different (more dissipative) layer conformation observed in the QCM-D experiments. The presence of grafted PEG chains on the molecule decreased the adsorption rate (but not the final adsorbed mass) on CNF and yielded less dissipative adsorbed layers than GGhydHox. GGM had good affinity for CNF, forming more rigid (less dissipative) adsorbed layers than the other polysaccharides, probably due to its smaller water uptake. It has previously

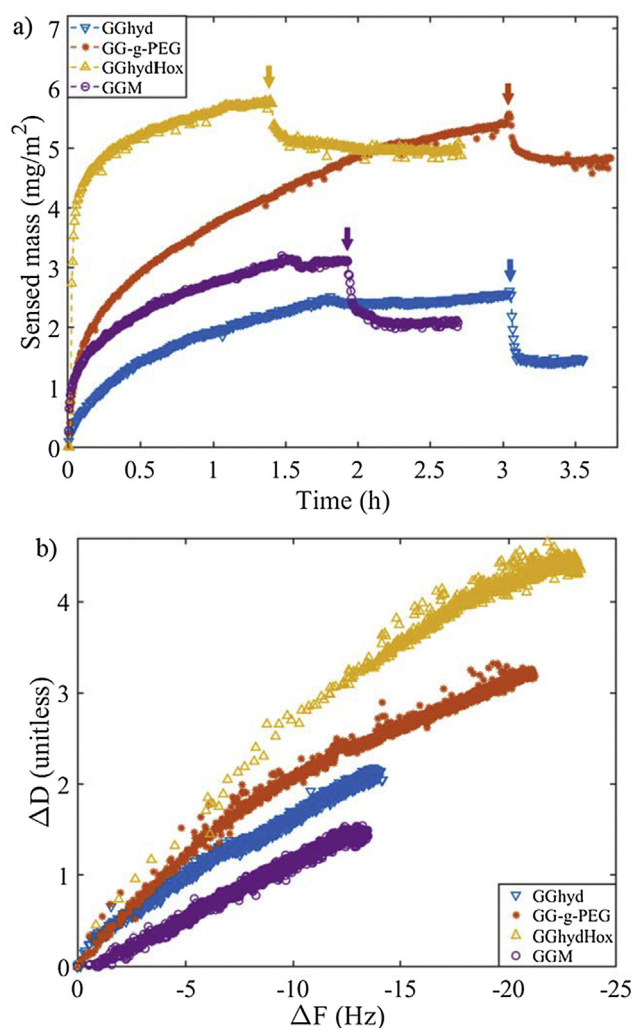


Fig. 2. Adsorption of different polysaccharides on CNF thin films: (a) sensed mass versus time (downward arrows indicate the point where rinsing with buffer started); (b) corresponding dissipation curves (change in dissipation vs change in frequency).

been found that aerogels from CNF and GGM can retain their shape in water [37], supporting the probability that GGM decreases the water sensitivity of CNF materials. Hydrolyzed GG was measured for comparison. The adsorbed mass of hydrolyzed GG was a bit lower than for other polysaccharides, due to its lower molecular weight. The effect of oxidation on the molecular weight of GG has been studied earlier [38]; the oxidation always increased the Mw and led to an increase in viscosity. In all cases, partial detachment of the polysaccharides from the CNF films was observed after rinsing with buffer (Fig. 2a).

Generally, it has been noted that, in its natural state, hemicellulose adsorbs irreversibly both on nanocellulose and on other hemicelluloses [3]. Also it has been noticed that although the molecular weight of the hemicellulose molecules affect the adsorption behavior, the side groups of the hemicellulose play a crucial role.

The adsorption behavior observed for GGM in this work is, in general, well in line with previous studies, in spite of the difference in GGM origin and molecular weights [39,17,40]. Eronen et al. observed that GGM adsorbed on both softwood and hardwood CNF in water with similar adsorption profiles as in Fig. 2, including partial detachment after rinsing [39]. Nevertheless, the GGM adsorbed masses were lower than in the present study, probably affected by the lower GGM concentration used in their experiments (100 mg/L vs. 300 mg/L). Lozhechnikova et al. noticed that GGM modification by the attachment of hydrophobic tails (fatty acids or polydimethylsiloxane) did not prevent adsorption on CNF [40]. Compared to our results, similar adsorbed masses and partial detachment after rinsing were reported for their unmodified GGM. On the other hand, TEMPO-oxidation of GGM has been shown to affect the adsorption on CNF: the adsorption of highly oxidized GGM was remarkably lower than unmodified GGM in water, but not in 0.1 M NaCl [17]. Unlike TEMPO oxidation, which introduces carboxyl groups to GGM, the enzymatic oxidation applied to GGhyd in our work enhanced the polysaccharide adsorption on CNF. Adsorption profiles on CNF qualitatively similar to the ones for GGM have also been observed for xyloglucan, which is another nonionic polysaccharide [39]. The adsorption of GG and GG degraded by acid hydrolysis (GG_{deg}) on CNF was also studied by Eronen et al. in 10 mM acetate buffer, pH 4.5 [23]. The adsorption and dissipation curves of GG_{deg} on CNF were quite similar to the ones for GGhyd obtained in our work, in spite of the different preparation method and molecular weight of the polysaccharides. Unmodified GG has been reported before not to improve the tensile strength of CNF composites [12], and therefore, it was not considered interesting for further study here.

Anionic, highly charged carboxymethyl cellulose (CMC) and a derivative prepared by grafting PEG chains to CMC (CMC-g-PEG) have been shown to adsorb on CNF in acetate buffer, pH 4.5 [41]. The corresponding adsorbed masses (2.3 mg/m² and 1.75 mg/m² for CMC and CMC-g-PEG, respectively) were clearly lower than for the nonionic (or residually charged) GG-g-PEG studied here, indicating that the polymer charge influences the adsorption on slightly anionic CNF. The adsorbed CMC and CMC-g-PEG layers were also more dissipative than the GG-g-PEG ones, showing that CMC and CMC-g-PEG adsorbed on CNF in a more extended, water-swollen conformation than GG-g-PEG. Another anionic hemicellulose, xylan, was also observed to have some affinity for CNF but also to form water-swollen, dissipative layers due to the repulsion between negative charges [41].

3.2. Interaction forces between cellulose and hemicellulose

In order to better understand the cellulose-cellulose, cellulose-hemicellulose, and hemicellulose-hemicellulose interactions during the formation of composite films, the surface forces between the cellulose surfaces and different polysaccharide layers at

micro/nanoscale were measured by colloidal probe microscopy. The measurements were carried out with two different setups. Cellulose-hemicellulose interactions were measured between cellulose colloidal probes and polysaccharide layers (GGhydHox, GG-g-PEG and GGM) previously adsorbed on CNF-coated QCM-D crystals. Cellulose-cellulose and hemicellulose-hemicellulose interactions were measured between cellulose colloidal probes and CNF-coated QCM-D crystals before and after the adsorption of polysaccharides (GG-g-PEG, GGM) *in situ*, in the AFM liquid cell.

A representative approach force curve between the cellulose surfaces (a cellulose colloidal probe and a CNF thin film before polysaccharide adsorption) is presented in Fig. 3. That force curve is well described by DLVO theory, as previously observed [42,43,41]. According to DLVO theory, the interaction force between a planar surface (CNF film) and a spherical particle (colloidal probe) of radius R can be described as the sum of the double layer repulsion and van der Waals attraction:

$$\frac{F(D)}{R} = 4\pi\epsilon_r\epsilon_0\kappa\psi_{\text{eff}}^2 e^{-\kappa D} - \frac{A}{6D^2} \quad (3)$$

where A is the Hamaker constant for cellulose in water, 8.0×10^{-21} J [44], ϵ_0 is the permittivity of vacuum, ϵ_r is the relative permittivity of water, ψ_{eff} is the (effective) surface potential, and κ is the inverse of the Debye length, which can be defined according to Debye-Hückel theory as:

$$\kappa^{-1} = \sqrt{\frac{\epsilon\epsilon_0 k_B T}{2q^2 N_A I}} \quad (4)$$

where I is the ionic strength of the buffer, k_B is the Boltzmann constant, T is the temperature and q is the electron charge [45]. Eq. (3) satisfactorily fits the approach force curve between bare cellulose at separations between 5 and 18 nm for 12 mM buffer ($\kappa \approx 0.4 \text{ nm}^{-1}$ at room temperature).

Representative approach force curves for the interaction between cellulose surfaces after the *in situ* adsorption of GGM and GG-g-PEG are also presented in Fig. 3. Those force curves show a very long range repulsion—clearly different from DLVO prediction—due to electrosteric forces arising from the compression of the polysaccharide layers. Electrosteric forces are forces that are

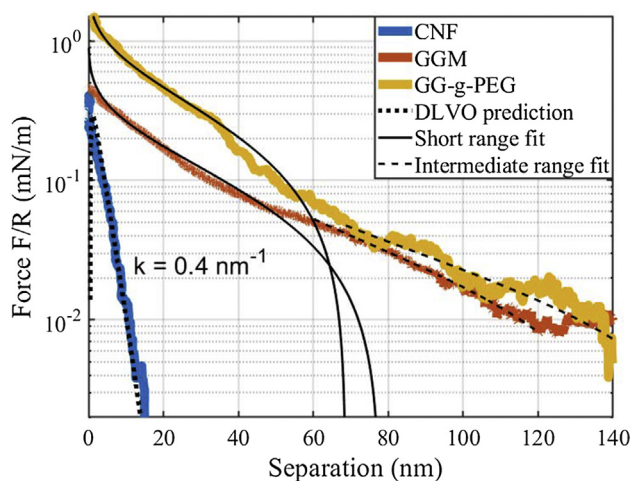


Fig. 3. Representative approach force curves between cellulose colloidal probes and CNF films before (blue) and after the adsorption of GGM (red) and GG-g-PEG (yellow) *in situ* in the AFM liquid cell. The DLVO prediction (dotted black line) was calculated for the known buffer ionic strength of 14 mM, which corresponds to an inverse Debye length of approx. 0.4 nm^{-1} . Solid and dashed lines correspond to the fits of the short and intermediate regimes of the polyelectrolyte brush model, respectively. (For interpretation of the references to color in this figure legend, the reader is referred to the web version of this article.)

due to both electrostatic and steric repulsion. The observed repulsion was well described by the polyelectrolyte brush model, [46,47] where two regimes at short and intermediate separation can be distinguished:

$$\frac{F(D)}{R} = 4\pi k_B T \left(\frac{d^2}{N_f} \right)^{-1} \log \left(\frac{2L}{D} \right); \quad \text{for } D < 2L \quad (5)$$

$$\frac{F(D)}{R} = \frac{\pi k_B T}{C_{\text{buf}} N_A} \left(\frac{d^2}{N_f} \right)^{-2} \left(\frac{1}{D} - \frac{1}{D^*} \right); \quad \text{for } 2L \leq D \leq D^* \quad (6)$$

where L is the thickness of the brush layer (brush length), $\frac{d^2}{N_f}$ is the area per charge of the brushed surfaces, C_{buf} is the concentration of the buffer, and N_A is the Avogadro's constant. The intermediate repulsion cut-off separation is D^* . These equations apply for the case where both surfaces are covered with polyelectrolyte brushes. In the case of force curves between a bare cellulose colloidal probe and polysaccharide layers previously adsorbed on CNF films (Fig. 4), Eqs. (5) and (6) can be used after replacing $2L$ with L . The corresponding brush lengths L obtained in the fits are presented in Tables 1 and S1.

The polyelectrolyte brush model has previously been applied to describe the interactions between surfaces coated with xylan, a negatively charged hemicellulose [46]. Although the polysaccharides used in this work are considered nonionic, the raw materials are known to have some impurities that provide a low residual charge. For example, GGM raw material contains 4% galactogluconic acid, 1% glucuronic acid, 0.2% 4-o methyl glucuronic acid and also other sugars like 1% xylose [25]. GG is known to contain 5–6% proteins [48], and its oxidation generates carboxyl groups that give a small residual charge. Parikka et al. [38] reported that 90–100% of galactosyls convert to carboxyl groups, when the total oxidation degree of the sample was 28–40%. The residual charge of GGM and GG justifies the use of the polyelectrolyte brush model to fit the force data.

Comparison of the mechanical tests indicated that longer polysaccharide brushes seemed to be beneficial for the macroscopic tensile strength and toughness of the cellulose-hemicellulose composites. In the samples adsorbed *in situ* in AFM the average brush length was 1.8 times higher for GGM compared

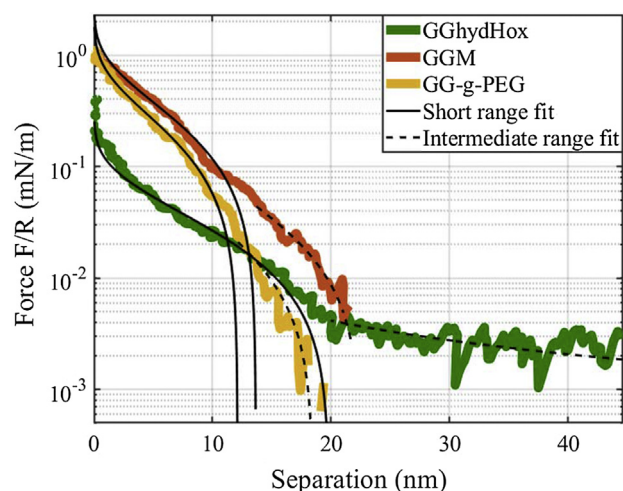


Fig. 4. Representative approach force curves between cellulose colloidal probes and GGhydHox (green), GGM (red), and GG-g-PEG (yellow) layers pre-adsorbed on CNF films in QCM-D experiments. Solid and dashed lines correspond to the fits of the short and intermediate regimes of the polyelectrolyte brush model, respectively. (For interpretation of the references to color in this figure legend, the reader is referred to the web version of this article.)

Table 1
Brush lengths of polysaccharide layers in different force experiments.

Sample	Adsorbed in	Average brush length L [nm]	Std. error of the mean [nm]
GGM	AFM	44.0	1.9
GG-g-PEG		24.0	1.4
GGhydHox	QCM-D	16.0	1.5
GGM		13.0	0.6
GG-g-PEG		12.0	0.7

to GG-g-PEG. Also for the samples pre-adsorbed in QCM-D, the average brush length was lowest for GG-g-PEG with a clear difference to GGhydHox which had a 1.3 times higher value for average brush length. The effect of compression of the polymers can be seen as an increase in the slope of the approaching force curves (Figs. 3 and 4). The electrosteric repulsion dominates the interactions between polysaccharide-polysaccharide layers and between cellulose-polysaccharide layers, preventing the detection of van der Waals forces, in line with previous works [42,46].

As can be seen in Table 1, the values of L were larger when the polysaccharides were adsorbed *in situ* (Fig. 3) than when they were preadsorbed (Fig. 4). In the former case, the adsorbed polymer layers were never dried during the force experiments, while, in the latter case, the substrates with the adsorbed polysaccharide were rinsed and dried under flowing nitrogen after the corresponding QCM-D adsorption experiment, a procedure that collapsed the brushes to some extent; they did not regain the same extended conformation upon rewetting.

While negligible adhesion was observed between bare cellulose surfaces upon retraction, a weak adhesion was detected between polysaccharide-polysaccharide and cellulose-polysaccharide layers (Fig. S4 and Table S2). Thus, the average percentage of force curves showing adhesion (and the corresponding maximum pull-off forces) were the following: $60\% \pm 10\%$ (-0.05 mN/m) and $20\% \pm 5\%$ (-0.06 mN/m) for GGM – GGM and cellulose – GGM, respectively; about 6% (-0.07 mN/m) and $35\% \pm 12\%$ (-0.07 mN/m) for GG-g-PEG – GG-g-PEG and cellulose – GG-g-PEG, respectively; and $70\% \pm 10\%$ (-0.07 mN/m) for cellulose – GGhydHox. Although the maximum pull-off forces were quite similar for all the systems, the probability of adhesion was in general higher for GGM and GGhydHox than for GG-g-PEG in the polysaccharide-polysaccharide interaction setup (adsorption *in situ* in AFM).

The interaction forces between cellulose surfaces coated with CMC and CMC-g-PEG have been previously measured by Olszewska, Junka et al. [41]. The electrosteric repulsion generated by CMC adsorption was pH-dependent due to the carboxylic groups of the polymer. The grafting of PEG chains of 2 kDa molecular weight (smaller than the 5 kDa PEG chains used in this work) remarkably increased the magnitude and range of the electrosteric repulsion in that case. Both the charge of the backbone polymer (highly charged CMC *versus* nonionic or residually charged GG) and the PEG grafting density (higher for CMC-g-PEG than for GG-g-PEG) are crucial factors that explain why much stronger electrosteric repulsions were observed between CMC-g-PEG layers than between the GG-g-PEG layers in this study. The range of forces was much larger than for the films with hemicelluloses. This is because GGM and GGhydHox are neutral polymers and CMC is charged. Xylan on CNF has been studied previously [46] and surface forces followed the polyelectrolyte brush force model and the adhesion was small, similarly as in our hemicellulose composites.

The method how the hemicellulose was adsorbed and how the sample was dried had relevant effects on the results. As the surfaces dry, the range of force decreases. The range of forces was

much smaller for the dried films with hemicelluloses. The CNF surfaces had always been dried before the adsorption of hemicellulose or force and friction measurements in AFM. However, the shape of force curves stayed relatively the same. The measured forces from CNF and hemicelluloses are small as the polymers are not highly charged.

3.3. Effect of adsorption of modified hemicelluloses on friction forces

Representative friction-*versus*-applied load curves between cellulose colloidal probes and CNF films before and after the adsorption of GGhydHox, GG-g-PEG and GGM are presented in Fig. 5. All

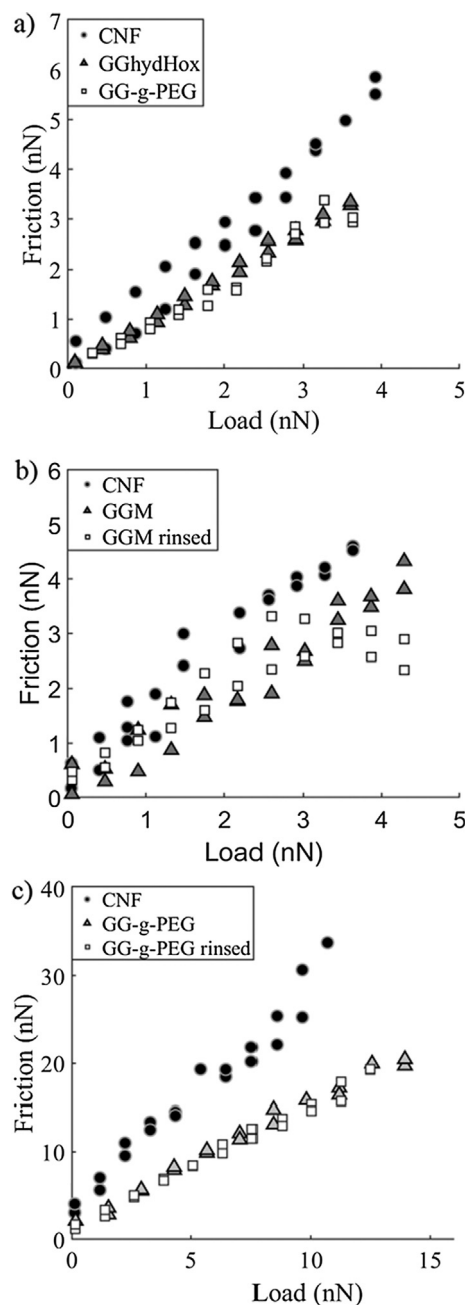


Fig. 5. Friction forces at different applied loads in different systems. (a) Friction forces between a cellulose colloidal probe and a CNF film without and with GGhydHox and GG-g-PEG adsorbed in QCM-D. (b) and (c) Friction forces between a cellulose colloidal probe and a CNF film before and after adsorbing GGM and GG-g-PEG, respectively, *in situ* in the AFM, and after rinsing with buffer.

the studied polysaccharides lowered the friction coefficient between cellulose surfaces by 12–41%, either when they adsorbed on just one surface (Fig. 5a) or on both (Fig. 5b and c). For instance, GGhydHox decreased the cellulose–CNF friction coefficient from 1.44 ± 0.12 to 0.97 ± 0.05 after adsorbing on CNF films, whereas GGM slightly reduced the cellulose–CNF friction coefficient from 1.15 ± 0.01 to 1.06 ± 0.02 after adsorbing on both the cellulose probe and the CNF film. The GG-g-PEG adsorbed *in situ* had the strongest lubricating effect, showing that even a very small amount of PEG chains affect friction. Rinsing with buffer to remove the non-properly attached polysaccharide molecules did not affect the lubrication provided by GGM and GG-g-PEG (Fig. 5b and c). Different friction forces and coefficients for cellulose–CNF were obtained when different cellulose colloidal probes were used. This phenomenon, probably due to differences in roughness between the cellulose probes, has been observed before [42]. In any case, there was a systematic decrease in both friction forces and friction coefficients after polysaccharide adsorption. The adsorption of polysaccharides did not change the roughness of the CNF films (Fig. S5), but the thin, soft layer that they formed on the cellulose surfaces had some lubricating effect.

It must be noted that the lubrication effect of the polysaccharides studied in this work is moderate. A much more pronounced lubrication effect was previously observed for CMC-g-PEG [41]. In contrast to GG-g-PEG, the high charge of CMC favors the swelling of CMC-g-PEG layers (in a pH-dependent manner), leading to stronger electrosteric repulsions and very efficient hydration lubrication. Therefore, it can be concluded that the polymer charge, together with the PEG grafting density, plays a crucial role in polymer-mediated lubrication.

3.4. Mechanical properties of free standing cellulose films

Plant-based CNF is a renewable, biodegradable, abundant, and lightweight material with good mechanical properties and high surface area. Because of that, CNF is a very interesting material for applications like packaging or barrier films. Previously we reported that the addition of various polysaccharides can enhance the tensile strength of CNF composites [12]. Especially, the wet strength of CNF films was improved considerably using oxidized GG and unmodified GGM. Here we sought an explanation for this effect by correlating interfacial interactions with wet strength, and to further extend the study to composites including GG-g-PEG and PEG. Tensile strength, Young's modulus and toughness of CNF-PEG and CNF-GG-g-PEG composites in wet and dry state are compared to previously published values for CNF-GGhydHox and CNF-GGM composites (Figs. 6 and S6).

The mechanical properties of CNF composites depend on the strength of the nanofibers, which is affected by the crystallinity and the degree of polymerization, and the interfibrillar interactions (surface and friction forces). In pure CNF films, single fibrils are in contact with numerous other fibrils, held together by hydrogen bonds and van der Waals forces. The CNF used in this study was from a fresh batch, which produced stronger CNF films than measured earlier using an older batch (Figs. 6 and S6). Aging, therefore, seems to have detrimental effect on CNF properties, possibly due to the formation of aggregates that are difficult to redisperse, or a decrease in the strength of individual nanofibers from a reduction in the degree of polymerization and, consequently, on the mechanical properties of the composites. Hence, the references for each batch are shown in the figures. The addition of polysaccharides can affect the interactions between CNF fibrils both during (e.g. by facilitating the even distribution of fibrils) and after (e.g. by mitigating crack propagation under stress) composite formation, which has direct consequences on the macroscopic mechanical properties of the composites.

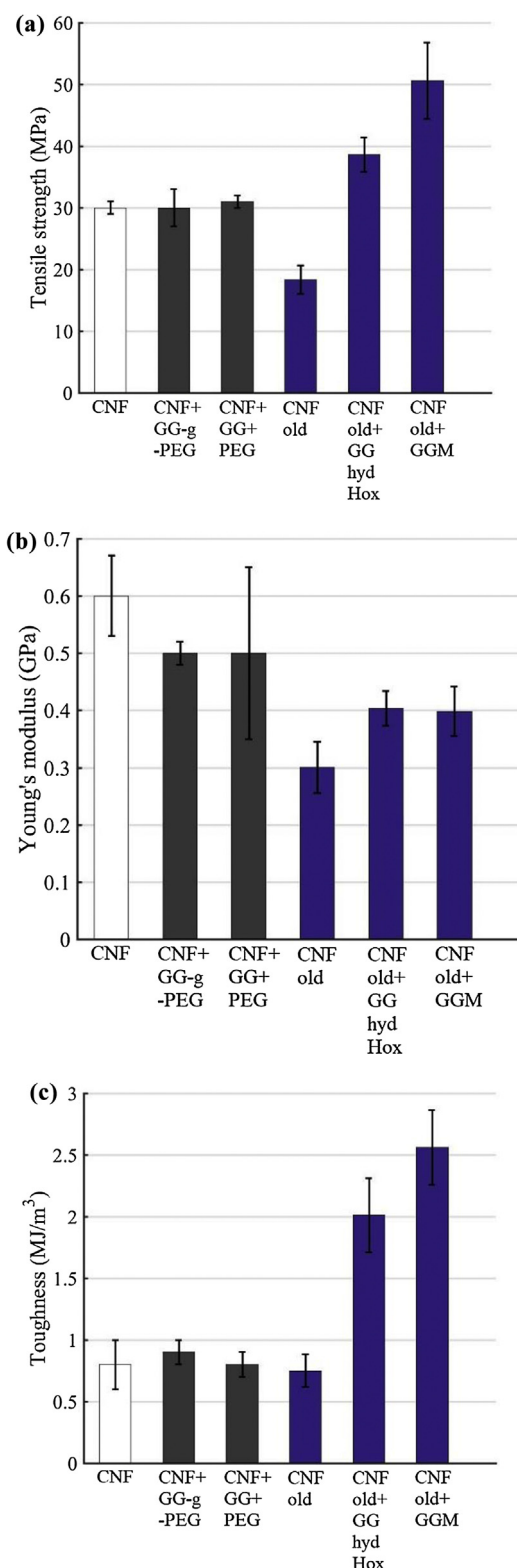


Fig. 6. Characterization of tensile mechanical properties of CNF-hemicellulose composites. The (a) tensile strength, (b) Young's modulus and (c) toughness of different composite films after being soaked in water for 24 h. The sample CNF + GG-g-PEG was dialyzed before mixing with CNF.

The addition of either GG or GGM to CNF has proven beneficial for composite toughness and tensile strength [49], especially in the wet state [12]. In dry conditions (Fig. S6), the tensile strength was improved by 60% and 50% with 2% addition of GGM, and of

GGhydHox respectively. The toughness increased by 360% and 270% with GGM and GGhydHox, respectively, but no clear effect on the Young's modulus was observed. Considering that only a very small decrease in friction was observed between a cellulose bead and a pre-adsorbed polysaccharide coated CNF film, this increase is not due to a lubricating effect, in contrast to previous observations for highly anionic polysaccharides [43]. These data are in line with previous results obtained for stacked epoxy CNF films, where the addition of 2% GGM improved the tensile strength by 31% and toughness by 100% [50]. The improvement in mechanical properties of the CNF composites was most pronounced in the wet state, after soaking the samples in water for 24 h (Fig. 6). The tensile strength increased by 170% and 100%, and the toughness augmented by 250% and 170%, after adding 2% GGM and GGhydHox, respectively. A moderate increase of 33% in the Young's modulus of the CNF composites in wet conditions was observed after adding the polysaccharides.

The addition of GG-g-PEG did not improve the mechanical properties of CNF composites in wet state, nor the addition of free PEG molecules (Fig. 6). Nevertheless, introducing GG-g-PEG in CNF composites provokes a slight increase in tensile strength, toughness and Young's modulus in the dry state (Fig. S6). Effective mixing of the components and even distribution of fibrils are essential when preparing freestanding CNF composite films. The moderate lubrication provided by GG-g-PEG can facilitate the even distribution of CNF fibrils in the final composite, improving, to some extent, the mechanical properties in dry conditions. However, unlike GGhydHox, GG-g-PEG did not enhance the mechanical properties of CNF composites in wet state, suggesting that the presence of hydrated PEG chains is not beneficial in wet conditions. In line with our results, highly lubricating CMC-g-PEG has been shown to increase the strength of CNF composites in dry conditions [43], but wet conditions have not been studied. Therefore, swelling (either due to polymer charge or hydration of hydrophilic molecules) has a negative effect on wet strength, as previous works have pointed out [51,52]. On the other hand, stretching CNF composites with grafted PEG chains has been reported to facilitate fibril alignment and, consequently, to improve the dry state strength of CNF-based ribbons [53] in the direction of alignment. Here we confirmed that the simple mixing of CNF and PEG did not significantly improve the mechanical properties of CNF composites either in dry or wet conditions.

Compared to GG-g-PEG, adsorbed GGM provided only moderate lubrication. The GGM layer had smaller water uptake, as can be seen by the lower dissipation at a similar change in frequency observed in the QCM-D adsorption experiments (Fig. 2). The lower water uptake together with moderate lubrication of GGM could explain the improved mechanical strength and toughness of CNF-GGM composites both in dry and wet states. The enhancing effect of GGM on the mechanical properties of CNF gels has also been reported by Prakobna, Kisonen et al. [52]. A similar mechanism could also explain the improvement in mechanical properties imparted by GGhydHox. The dissipative nature of the GGhydHox adsorbed layer observed in QCM-D experiments could be due to the crosslinking and gel formation of GGhydHox on top of CNF films, and not swelling due to water uptake, explaining the positive effect on wet strength. In fact, hydrolyzed oxidized galactoglucomannans can form strong hydrogels and aerogels. Alakalunmaa et al. observed that adding CNF improved the mechanical properties, but oxidized galactoglucomannans could actually form gels on their own [37].

It is worth to mention the work by Mautner et al. [54] where they studied films made of different type of nanocelluloses, e.g. bacterial cellulose (BC), cellulose nanocrystals (CNC), and TEMPO oxidized-CNF. They noticed that nanocellulose mixtures have syn-

ergistic effects on tensile properties. For instance, CNC can be used to fill the voids between larger BC ribbons in BC-nanopapers.

No common standards are available for testing different kinds of CNF films, which makes comparison of the results difficult, since the size of the specimen and the testing speed highly affect the results. We used relatively large samples, keeping practical applications in mind, such as in medicine (artificial skin or blood vessels), packing, sensors and electronics [13]. The ability to practically transfer the good properties of CNF materials to real samples is often questioned. Therefore, we did not want to optimize the testing setup to obtain high tensile strength results, but rather tested larger samples, although the risk of including defects is larger [9].

The combined information about the viscoelasticity of the adsorbed polysaccharide layers, the surface forces suggesting a polyelectrolyte brush conformation of the polymers, and the effect on friction forces gave valuable information about how these water-soluble polysaccharides interact with cellulose. This can be used to understand the interactions between these components in the plant cell wall, and how these interactions affect the strength of hydrogels or composites made from these, enabling optimization of these properties.

4. Conclusions

The interactions between hemicellulose and cellulose nanofibrils (CNF) and fibers play an important role in the structure and mechanical properties of wood. The main aim of this work was to better understand these hemicellulose-cellulose interactions, and to correlate those interactions with the mechanical properties of CNF-hemicellulose composites. CNF is an abundant, natural, renewable, biodegradable material, and more economical than other possible fillers like graphene or carbon nanotubes. Thus, cellulose-hemicellulose composites were prepared by combining CNF with different modified and unmodified polysaccharides (GGM, GGhydHox, and GG-g-PEG). The affinities and interactions of CNF-polysaccharides were quantified by QCM-D and AFM colloidal probe microscopy, respectively, and the results were correlated to the mechanical properties of free-standing films in wet and dry state. Although all the polysaccharides tested adsorbed well on CNF, GGhydHox adsorbed with the fastest rate. The presence of grafted PEG chains on the hydrolyzed-oxidized guar gum molecule decreased the rate of adsorption on CNF. Compared to the adsorption of anionic carboxymethyl cellulose with grafted PEG chains (CMC-g-PEG) [41], GG-g-PEG was observed to adsorb on CNF in a higher amount, and forming a less dissipative layer. Furthermore, repulsive interactions of lower range and higher friction were measured between GG-g-PEG coated cellulose substrates, showing the effect of the backbone polymer charge (anionic, highly charged CMC *versus* practically nonionic GG) on the adsorption on CNF, and on the corresponding surface and friction forces. On the other hand, the adsorption of GGM on CNF was, in general, well in line with previous studies [39,17,40]. GGM had good affinity for CNF, forming less dissipative adsorbed layers compared to the other tested polysaccharides, probably because of its smaller water uptake. The repulsive forces measured when approaching polysaccharide-coated cellulose surfaces were well described by the polyelectrolyte brush model, with longer brush lengths obtained for GGM than for GG-g-PEG. The polysaccharides studied lowered the friction coefficient between cellulose surfaces by 12–41% upon adsorption on one or on both interacting surfaces. In general, long-range repulsion and moderate lubrication correlated with improved mechanical properties of the composites in dry state, probably because the polysaccharide-mediated

interactions facilitate the even distribution of CNF during composite formation. On the other hand, the polysaccharide's swelling (hydration) capacity negatively affected the strength of CNF-based composites in wet conditions. Thus, GGM, which did not bind as much water as GG-g-PEG, improved the wet strength of CNF films, but GG-g-PEG did not. Overall, the results shed light on how different types of polysaccharides adsorb on cellulose and how they affect the interfacial interactions. This enhances our understanding of the interactions between cellulose and hemicelluloses in the cell wall of plants as well as their interactions in hydrogels and composites enabling optimization of properties.

Acknowledgements

J.L. thanks the Foundation for Research of Natural Resources in Finland (project number 2014069), Aalto University, and Finnish Forest Products Engineers for funding, and Dr. Nikolas Pahimanolis for his help in operating the NMR device. M.Sc. Muhammad Farooq is acknowledged for helping in the preparation of the graphical abstract.

Appendix A. Supplementary material

Supplementary data to this article can be found online at <https://doi.org/10.1016/j.jcis.2019.07.053>.

References

- [1] K.S. Mikkonen, Recent studies on hemicellulose-based blends, composites and nanocomposites, in: *Advances in Natural Polymers*, Springer, 2013, pp. 313–336.
- [2] S. Mondal, Preparation, properties and applications of nanocellulosic materials, *Carbohydr. Polym.* 163 (2017) 301–316.
- [3] T. Tammelin, A. Paananen, M. Österberg, *Hemicelluloses at Interfaces: Some Aspects of the Interactions*, Wiley-Blackwell Publishing Ltd, Chichester, 2009.
- [4] N. Nordgren, P. Eronen, M. Österberg, J. Laine, M.W. Rutland, Mediation of the nanotribological properties of cellulose by chitosan adsorption, *Biomacromolecules* 10 (3) (2009) 645–650.
- [5] P. Eronen, J. Laine, J. Ruokolainen, M. Österberg, Comparison of multilayer formation between different cellulose nanofibrils and cationic polymers, *J. Colloid Interface Sci.* 373 (1) (2012) 84–93.
- [6] T. Tenhunen, M.S. Peresin, P.A. Penttilä, J. Pere, R. Serimaa, T. Tammelin, Significance of xylan on the stability and water interactions of cellulosic nanofibrils, *React. Funct. Polym.* 85 (2014) 157–166.
- [7] B. Derjaguin, L. Landau, Theory of the stability of strongly charged lyophobic sols and of the adhesion of strongly charged particles in solution of electrolytes, *Acta Physicochim. U.S.S.R.* 14 (1941) 633–662.
- [8] E. Verwey, J.T.G. Overbeek, *Theory of Stability of Lyophobic Colloids*, Elsevier Publishing Co., 1948.
- [9] E. Kontturi, P. Laaksonen, M.B. Linder, Nonappa, A.H. Gröschel, O.J. Rojas, O. Ikkala, Advanced materials through assembly of nanocelluloses, *Adv. Mater.* 30 (2018) 1703779.
- [10] M.A. Hubbe, A. Ferrer, P. Tyagi, Y. Yin, C. Salas, L. Pal, O.J. Rojas, Nanocellulose in thin films, coatings, and plies for packaging applications: a review, *BioResources* 12 (1) (2017) 2143–2233.
- [11] W. Farhat, R.A. Venditti, M. Hubbe, M. Taha, F. Becquart, A. Ayoub, A review of water-resistant hemicellulose-based materials: processing and applications, *ChemSusChem* 10 (2) (2017) 305–323.
- [12] J. Lucenius, K. Parikka, M. Österberg, Nanocomposite films based on cellulose nanofibrils and water-soluble polysaccharides, *React. Funct. Polym.* 85 (2014) 167–174.
- [13] A. Benítez, A. Walthner, Cellulose nanofibril nanopapers and bioinspired nanocomposites: a review to understand the mechanical property space, *J. Mater. Chem. A* 5 (31) (2017) 16003–16024.
- [14] A.J. Svagan, M.A. Azizi Samir, L.A. Berglund, Biomimetic polysaccharide nanocomposites of high cellulose content and high toughness, *Biomacromolecules* 8 (8) (2007) 2556–2563.
- [15] H. Sehaqui, Q. Zhou, L.A. Berglund, Nanostructured biocomposites of high toughness—a wood cellulose nanofiber network in ductile hydroxyethylcellulose matrix, *Soft Matter* 7 (16) (2011) 7342–7350.
- [16] P. Fratzl, R. Weinkamer, Nature's hierarchical materials, *Prog. Mater. Sci.* 52 (8) (2007) 1263–1334.
- [17] A. Leppänen, C. Xu, P. Eklund, J. Lucenius, M. Österberg, S. Willför, Targeted functionalization of spruce O-acetyl galactoglucomannans—2, 2, 6, 6-tetramethylpiperidin-1-oxyl-oxidation and carbodiimide-mediated amidation, *J. Appl. Polym. Sci.* 130 (5) (2013) 3122–3129.
- [18] Z. Shi, C. Jia, D. Wang, J. Deng, G. Xu, C. Wu, M. Dong, Z. Guo, Synthesis and characterization of porous tree gum grafted copolymer derived from *Prunus cerasifera* gum polysaccharide, *Int. J. Biol. Macromol.* 133 (2019) 964–970.
- [19] L. Zhao, J. Li, L. Zhang, Y. Wang, J. Wang, B. Gu, J. Chen, T. Hao, C. Wang, N. Wen, Preparation and characterization of calcium phosphate/pectin scaffolds for bone tissue engineering, *RSC Adv.* 6 (67) (2016) 62071–62082.
- [20] K. Parikka, M. Tenkanen, Oxidation of methyl α -D-galactopyranoside by galactose oxidase: products formed and optimization of reaction conditions for production of aldehyde, *Carbohydr. Res.* 344 (1) (2009) 14–20.
- [21] A. Ghafar, P. Gurikov, R. Subrahmanyam, K. Parikka, M. Tenkanen, I. Smirnova, K.S. Mikkonen, Mesoporous guar galactomannan based biocomposite aerogels through enzymatic crosslinking, *Compos. A Appl. Sci. Manuf.* 94 (2017) 93–103.
- [22] A. Swerin, L. Ödberg, T. Lindström, Deswelling of hardwood kraft pulp fibres by cationic polymers. The effect on wet pressing and sheet properties, *Nord. Pulp Pap. Res. J.* 5 (4) (1990) 188–196.
- [23] P. Eronen, K. Junka, J. Laine, M. Österberg, Interaction between water-soluble polysaccharides and native nanofibrillar cellulose thin films, *BioResources* 6 (4) (2011) 4200–4217.
- [24] P. Eronen, *Adsorption Studies on Cellulose Surfaces by Combinations of Interfacial Techniques*, Aalto University, 2011.
- [25] C. Xu, S. Willför, K. Sundberg, C. Pettersson, B. Holmbom, Physico-chemical characterization of spruce galactoglucomannan solutions: stability, surface activity and rheology, *Cellul. Chem. Technol.* 41 (1) (2007) 51.
- [26] K. Parikka, A. Leppänen, L. Pitkänen, M. Reunanen, S. Willför, M. Tenkanen, Oxidation of polysaccharides by galactose oxidase, *J. Agric. Food. Chem.* 58 (1) (2009) 262–271.
- [27] T.L. Schlick, Z. Ding, E.W. Kovacs, M.B. Francis, Dual-surface modification of the tobacco mosaic virus, *J. Am. Chem. Soc.* 127 (11) (2005) 3718–3723.
- [28] A. Richard, A. Barras, A.B. Younes, N. Monfiliette-Dupont, P. Melynyk, Minimal chemical modification of reductive end of dextran to produce an amphiphilic polysaccharide able to incorporate onto lipid nanocapsules, *Bioconjug. Chem.* 19 (7) (2008) 1491–1495.
- [29] M. Österberg, J. Vartiainen, J. Lucenius, U. Hippo, J. Seppälä, R. Serimaa, J. Laine, A fast method to produce strong NFC films as a platform for barrier and functional materials, *ACS Appl. Mater. Interfaces* 5 (11) (2013) 4640–4647.
- [30] S. Ahola, J. Salmi, L. Johansson, J. Laine, M. Österberg, Model films from native cellulose nanofibrils. Preparation, swelling, and surface interactions, *Biomacromolecules* 9 (4) (2008) 1273–1282.
- [31] E. Kontturi, P.C. Thüne, J. Niemantsverdriet, Cellulose model surfaces simplified preparation by spin coating and characterization by X-ray photoelectron spectroscopy, infrared spectroscopy, and atomic force microscopy, *Langmuir* 19 (14) (2003) 5735–5741.
- [32] H. Orelma, I. Filpponen, L. Johansson, M. Österberg, O.J. Rojas, J. Laine, Surface functionalized nanofibrillar cellulose (NFC) film as a platform for immunoassays and diagnostics, *Biointerphases* 7 (1–4) (2012) 1–12.
- [33] W. Ducker, T. Senden, R. Pashley, Direct measurement of colloidal forces using an atomic force microscope, *Nature* 353 (1991) 239–241.
- [34] J. Ralston, I. Larson, M.W. Rutland, A.A. Feiler, M. Kleijn, Atomic force microscopy and direct surface force measurements (IUPAC technical report), *Pure Appl. Chem.* 77 (12) (2005) 2149–2170.
- [35] C.P. Green, H. Lioe, J.P. Cleveland, R. Proksch, P. Mulvaney, J.E. Sader, Normal and torsional spring constants of atomic force microscope cantilevers, *Rev. Sci. Instrum.* 75 (6) (2004) 1988–1996.
- [36] A.M. Olszewska, *Interfacial Forces in Nanocellulose Based Composite Materials*, Aalto University, 2013.
- [37] S. Alakhalunmaa, K. Parikka, P.A. Penttilä, M.T. Cuberes, S. Willför, L. Salmén, K. S. Mikkonen, Softwood-based sponge gels, *Cellulose* 23 (5) (2016) 3221–3238.
- [38] K. Parikka, A. Leppänen, C. Xu, L. Pitkänen, P. Eronen, M. Österberg, H. Brumer, S. Willför, M. Tenkanen, Functional and anionic cellulose-interacting polymers by selective chemo-enzymatic carboxylation of galactose-containing polysaccharides, *Biomacromolecules* 13 (8) (2012) 2418–2428.
- [39] P. Eronen, M. Österberg, S. Heikkinen, M. Tenkanen, J. Laine, Interactions of structurally different hemicelluloses with nanofibrillar cellulose, *Carbohydr. Polym.* 86 (3) (2011) 1281–1290.
- [40] A. Lozhechnikova, D. Dax, J. Vartiainen, S. Willför, C. Xu, M. Österberg, Modification of nanofibrillated cellulose using amphiphilic block-structured galactoglucomannans, *Carbohydr. Polym.* 110 (2014) 163–172.
- [41] A. Olszewska, K. Junka, N. Nordgren, J. Laine, M.W. Rutland, M. Österberg, Non-ionic assembly of nanofibrillated cellulose and polyethylene glycol grafted carboxymethyl cellulose and the effect of aqueous lubrication in nanocomposite formation, *Soft Matter* 9 (31) (2013) 7448–7457.
- [42] J. Stiernstedt, N. Nordgren, L. Wågberg, H. Brumer, D.G. Gray, M.W. Rutland, Friction and forces between cellulose model surfaces: A comparison, *J. Colloid Interface Sci.* 303 (1) (2006) 117–123.
- [43] A. Olszewska, J.J. Valle-Delgado, M. Nikinmaa, J. Laine, M. Österberg, Direct measurements of non-ionic attraction and nanoscaled lubrication in biomimetic composites from nanofibrillated cellulose and modified carboxymethylated cellulose, *Nanoscale* 5 (23) (2013) 11837–11844.
- [44] L. Bergström, S. Stemme, T. Dahlfors, H. Arwin, L. Ödberg, Spectroscopic ellipsometry characterisation and estimation of the Hamaker constant of cellulose, *Cellulose* 6 (1) (1999) 1–13.
- [45] G. Trefalt, I. Szilagy, M. Borkovec, Poisson-Boltzmann description of interaction forces and aggregation rates involving charged colloidal particles in asymmetric electrolytes, *J. Colloid Interface Sci.* 406 (2013) 111–120.

- [46] M. Österberg, J. Laine, P. Stenius, A. Kumpulainen, P.M. Claesson, Forces between xylan-coated surfaces: effect of polymer charge density and background electrolyte, *J. Colloid Interface Sci.* 242 (1) (2001) 59–66.
- [47] P. Pincus, Colloid stabilization with grafted polyelectrolytes, *Macromolecules* 24 (10) (1991) 2912–2919.
- [48] N. Thombare, U. Jha, S. Mishra, M.Z. Siddiqui, Guar gum as a promising starting material for diverse applications: a review, *Int. J. Biol. Macromol.* 88 (2016) 361–372.
- [49] K.S. Mikkonen, J.S. Stevanic, C. Joly, P. Dole, K. Pirkkalainen, R. Serimaa, L. Salmén, M. Tenkanen, Composite films from spruce galactoglucomannans with microfibrillated spruce wood cellulose, *Cellulose* 18 (3) (2011) 713–726.
- [50] A. Mautner, J. Lucenius, M. Österberg, A. Bismarck, Multi-layer nanopaper based composites, *Cellulose* 24 (4) (2017) 1759–1773.
- [51] N. Pahimanolis, A. Salminen, P.A. Penttilä, J.T. Korhonen, L. Johansson, J. Ruokolainen, R. Serimaa, J. Seppälä, Nanofibrillated cellulose/carboxymethyl cellulose composite with improved wet strength, *Cellulose* (2013) 1–10.
- [52] K. Prakobna, V. Kisonen, C. Xu, L.A. Berglund, Strong reinforcing effects from galactoglucomannan hemicellulose on mechanical behavior of wet cellulose nanofiber gels, *J. Mater. Sci.* 50 (22) (2015) 7413–7423.
- [53] H. Tang, N. Butchosa, Q. Zhou, A transparent, hazy, and strong macroscopic ribbon of oriented cellulose nanofibrils bearing poly (ethylene glycol), *Adv. Mater.* 27 (12) (2015) 2070–2076.
- [54] A. Mautner, F. Mayer, M. Hervy, K. Lee, A. Bismarck, Better together: synergy in nanocellulose blends, *Philos. Trans. Roy. Soc. A: Math. Phys. Eng. Sci.* 376 (2112) (2017) 20170043.